Published in final edited form as:
Tissue Eng Part A. 2008 November ; 14(11): 1809–1820. doi:10.1089/ten.tea.2007.0255.

Effects of Initial Seeding Density and Fluid Perfusion Rate on Formation of Tissue-Engineered Bone

WARREN L. GRAYSON, Ph.D.[1], **SARINDR BHUMIRATANA, M.S.**[1], **CHRISTOPHER CANNIZZARO, Ph.D.**[2], **P.-H. GRACE CHAO, Ph.D.**[1], **DONALD P. LENNON, Ph.D.**[3], **ARNOLD I. CAPLAN, Ph.D.**[3], and **GORDANA VUNJAK-NOVAKOVIC, Ph.D.**[1]

[1] Department of Biomedical Engineering, Columbia University, New York, New York

[2] Department of Biomedical Engineering, Tufts University, Medford, Massachusetts

[3] Skeletal Research Center, Department of Biology, Case Western Reserve University, Cleveland, Ohio

Abstract

We describe a novel bioreactor system for tissue engineering of bone that enables cultivation of up to six tissue constructs simultaneously, with direct perfusion and imaging capability. The bioreactor was used to investigate the relative effects of initial seeding density and medium perfusion rate on the growth and osteogenic differentiation patterns of bone marrow–derived human mesenchymal stem cells (hMSCs) cultured on three-dimensional scaffolds. Fully decellularized bovine trabecular bone was used as a scaffold because it provided suitable "biomimetic" topography, biochemical composition, and mechanical properties for osteogenic differentiation of hMSCs. Trabecular bone plugs were completely denuded of cellular material using a serial treatment with hypotonic buffers and detergents, seeded with hMSCs, and cultured for 5 weeks. Increasing seeding density from 30×10^6 cells/mL to 60×10^6 cells/mL did not measurably influence the characteristics of tissue-engineered bone, in contrast to an increase in the perfusion rate from 100 μms^{-1} to 400 μms^{-1}, which radically improved final cell numbers, cell distributions throughout the constructs, and the amounts of bone proteins and minerals. Taken together, these findings suggest that the rate of medium perfusion during cultivation has a significant effect on the characteristics of engineered bone.

INTRODUCTION

The ability to develop uniform bone constructs of clinically relevant sizes remains a challenge and depends on the ability to optimize various *in vitro* culture parameters. One limitation in the development of tissue-engineered bone grafts is the insufficient transport of nutrients—in particular oxygen—into the inner regions of the scaffolds.[1,2] Medium perfusion, therefore, is essential for constructs thicker than several hundred micrometers in order to provide convectional transport of nutrients and oxygen to all cells.[3,4] Prior studies of various three-dimensional (3D) scaffold systems seeded with osteoblasts or bone marrow–derived stem cells have demonstrated that medium perfusion through constructs enhance bone tissue formation[5–12] as a result of improved nutrient transfer and the intrinsic shear stresses associated with the medium flow. In 2D[13–15] and 3D[9,10] systems, shear forces—a physiologically relevant stimulus—have been shown to specifically influence the expression of osteogenic genes in osteoblasts. Cultivation of scaffolds with direct medium perfusion requires the development of specialized bioreactor systems. The bioreactor systems described in the

Address reprint requests to: Gordana Vunjak-Novakovic, Ph.D., Columbia University, Department of Biomedical Engineering, 622 West 168th Street VC12-234, New York, NY 10032, gv2131@columbia.edu.

literature[4,8,12] are able to culture only single 3D tissue constructs at a given time and do not provide imaging capability. We describe the development of an easy-to-use, novel bioreactor system that enables the cultivation of up to six tissue constructs simultaneously, with direct perfusion of culture medium and imaging throughout the period of cultivation.

Cell-seeding density is known to influence the characteristics and functionality of engineered tissues. In prior studies, the effect of varying the density of cells seeded into constructs was investigated for bone, cartilage, and cardiac tissues.[16–20] The effect of higher seeding densities was dependent on the tissue type as well as the culture conditions. For example, high seeding densities of chondrocytes in agarose gels yielded better mechanical properties, but these gels were less responsive to mechanical stimulation.[18] When the seeding density for tissue engineered bone was increased from 1×10^6 cells/mL to 10×10^6 cells/mL, there was no enhancement in bone formation.[19] However, homogenous cell distribution throughout the constructs, which facilitates tissue development, was better at higher seeding densities. Hence, there is a need to better understand the effects of the initial cell density and medium flow on bone formation to support the required construct development and functionality.

In this study mineralized, fully decellularized bone (DCB) was used to generate scaffolds for tissue-engineering applications. Prior studies, including the seminal work done by Urist,[21] have demonstrated the utility of demineralized bone matrix as an osteo-inductive biomaterial and have led to the discovery of bone-derived growth factors, the primary osteoinductive components of bone matrix.[22] As a result, various forms of demineralized bone matrix, bone morphogenetic proteins, and bone graft substitutes (including allografts) are now commonly used in clinical applications for bone repair.[23] We hypothesized that the ability of DCB grafts to provide the osteoinductive growth factors, in addition to mechanical, biochemical, and architectural properties, without eliciting immunogenic responses makes them a suitable scaffold for bone tissue–engineering applications. DCB also has a potential advantage over the commonly used demineralized bone matrix in that its superior mechanical properties can help to expedite its functionality upon integration into defects in load-bearing sites. DCB scaffolds have already been employed for various tissue-engineering applications.[24–27] However, here we describe the application of a rigorous technique for removing all of the cellular material from cores taken from the trabecular regions of bovine bone, with the aim of obtaining biological, osteoinductive, degradable scaffolds, which may be seeded with human mesenchymal stem cells (hMSCs) to tissue engineer bone grafts for the treatment of load-bearing, clinically relevant osseous non-unions.

To determine the relative contributions of perfusion rates and cell seeding density on the characteristics of tissue-engineered bone, a novel bioreactor system was developed, characterized, and used to investigate the effect of two different medium perfusion rates (superficial velocities through scaffold: 100 μms^{-1} and 400 μms^{-1}) and two seeding densities (30×10^6 cells/mL and 60×10^6 cells/mL). The growth and tissue development of hMSCs seeded into the DCB scaffolds and cultured for 5 weeks were evaluated using biochemical, histological, and imaging techniques. It was found that perfusion rates had greater influence on cell growth and bone formation than did the initial seeding density.

MATERIALS AND METHODS

Perfusion bioreactor

A novel, easy-to-use perfusion bioreactor system has been developed, which addresses several key design issues including the use of multiple scaffolds (4 to 10 mm in diameter and up to 4 mm high) and imaging capabilities. The bioreactor has the dimensions of a 10-cm glass Petri dish, and the glass cover of this dish serves as the removable bioreactor cover (Fig. 1A). This enables access to scaffolds as well as the use of traditional cell culture techniques for medium

changes, thus eliminating any technical challenges of using an engineering system for cell culture. The bioreactor was machined from polycarbonate plastic with medical-grade (platinum cured) silicone gaskets separating the individual parts. Scaffolds were press-fit in place into a layer of polydimethylsiloxane (PDMS).

Scaffolds were placed into six wells arranged in a radial pattern. Medium entered the bioreactor through a central port from where it flowed to the center of the bioreactor and became evenly distributed into six channels leading to the scaffolds (Fig. 1B). The width and height of the inlet channel were 1.0 mm×1.0 mm. The six channels leading to each scaffold were 1.0 mm wide and had a height that was tapered from 1.0 mm at the center to 0.5 mm below each scaffold. The channels were designed to provide relatively high flow resistance to the medium recirculation, as opposed to the resistance provided by the scaffolds themselves, and thereby maintained equal flow rates of culture medium through each scaffold. To verify this important feature of the bioreactor, we measured the flow rate through scaffolds with different densities at a constant pressure head. In addition, the flow rate through the bioreactor with and without scaffolds were compared at high and low pressure heads. This measurement was repeated at multiple time points. In each case, the flow rate was determined by measuring the total time taken for 20 mL of fluid to flow through, and this measurement was repeated at multiple time points.

The bioreactor was checked for the formation of bubbles every day to avoid obstruction of flow. Any gas bubbles that formed in the channels were removed using a syringe attached upstream of the inlet port using a three-way connector. During normal operation, the syringe is closed off from the flow of medium. Medium from the space above the scaffolds, which serves as a reservoir, flows through the scaffolds. During culture, the direction of flow is upwards through the scaffold into the reservoir, which enables the use of the reservoir as a bubble trap. The reservoir also serves as a gas exchanger for equilibrating oxygen and pH levels in culture medium with the incubator environment. Medium flows out of the reservoir through a port on the side of the bioreactor and is re-circulated by a low-flow multi-channel digital peristaltic Ismatec pump (Cole-Parmer, Vernon Hills, IL).

Decellularized bone scaffolds

Cylindrical, trabecular bone grafts (4 mm in diameter) were cored from the subchondral region of carpometacarpal joints of 2-week- to 4-month-old cows. The plugs were washed with a high-velocity stream of water to remove the marrow from the pore spaces and then for 1 hr in phosphate buffered saline (PBS) with 0.1% ethylenediaminetetraacetic acid (EDTA) at room temperature. This step was followed by sequential washes in hypotonic buffer (10 mM Tris, 0.1% EDTA, overnight at 4°C), detergent (10 mM Tris, 0.5% sodium dodecyl sulfate (SDS), for 24 h at room temperature) and enzymatic solution (50 U/mL DNAse, 1 U/mL RNAse, 10 mM Tris, for 3–6 h at 37°C) to remove any remaining cellular material. After each step, the scaffolds were rinsed with PBS for 1 h. After SDS treatment, several washes (≥7) were performed until no more bubbles indicating the presence of detergent were seen in the PBS during washing. At the end of the process, decellularized bone plugs were rinsed in PBS, freeze-dried, and cut to 4-mm-long cylinders. The weights and exact dimensions of the plugs were measured and used to calculate the scaffold density and porosity. Scaffolds were sterilized in 70% ethanol for 1 h and incubated in culture medium overnight before seeding cells.

In vivo studies of scaffolds

To test for any immunogenic properties, decellularized bone scaffolds were implanted subcutaneously into the ventral regions of Sprague-Dawley rats following an approved standard protocol. The samples were removed 2 weeks after implantation, fixed in 3.7%

formaldehyde, demineralized, embedded in paraffin, and sectioned into 5-μm-thick slices. Slides were stained with hematoxylin and eosin.

Human mesenchymal stem cells

Bone marrow–derived hMSCs were isolated from bone marrow aspirates taken with donor consent during hip replacement surgeries, using previously described cell isolation methods.[28] Cells were culture expanded in low-glucose Dulbecco's Modified Eagle Medium (DMEM) supplemented with 10% fetal bovine serum and 1% penicillin-streptomycin (control medium) up to the fourth passage and were then used for seeding onto the scaffolds. Constructs were subsequently cultured with control medium supplemented with osteogenic supplements: 10 nM dexamethasone, 10 mM sodium-β-glycerophosphate, and 0.05 mM ascorbic acid-2-phosphate.

Construct seeding and culture

Cells at the fourth passage were resuspended at a low seeding density (LS) of 30×10^6 or a high seeding density (HS) of 60×10^6 cells/mL. A 50-μL aliquot of the cell suspension was pipetted to the top of blot-dried scaffolds and allowed to percolate through. After 15 min, the scaffolds were rotated 180°, and 10 μL of medium was added to prevent the cells from drying out. This process was repeated every 15 min for up to 2 h to facilitate uniform cell distribution. Constructs were then placed in the bioreactors, and 40 mL of medium was added. After 1 day, scaffolds were perfused at a superficial velocity of 10 μm/s for up to 1 week to provide local supply of oxygen to the cells while maintaining low hydrodynamic shear to promote cell attachment.

The medium flow rates were then set to provide the superficial velocity of medium through the scaffolds of 100 $\mu m/s^{-1}$ (low-flow; LF) or 400 μms^{-1} (high flow; HF). This resulted in four experimental groups: unseeded scaffolds (US) placed in bioreactors and perfused at 400 μms^{-1}, LS-LF, LS-HF, and HS-LF. During culture, 50% of the medium volume was replaced twice a week. This partial medium exchange was determined in previous studies to provide supply of fresh nutrients along with the maintenance of cell-secreted factors in the cell environment. After 4 weeks of culture, the constructs were harvested and cut in half and the wet weight of each half was determined. Four constructs were used to provide statistical evaluation of the DNA and protein contents and alkaline phosphatase activity. The two remaining constructs from each group were used for imaging (histology, scanning electron microscopy (SEM), and micro-computed tomography (μ-CT)). After fixation, samples were imaged using μ-CT, then half of each sample was used for histology, and the other half was used for SEM.

Analytical assays

DNA—Tissue constructs were washed in PBS and then placed in 100 μL of digestion buffer (10 mM Tris, 1 mM EDTA and 0.1% Triton X-100) with 0.1 mg/mL of proteinase K in micro-centrifuge tubes. Constructs were maintained in this solution overnight at 50°C. The supernatants were drawn off and diluted 10×. A standard curve was prepared from a solution of salmon testes DNA obtained from Molecular Probes (Eugene, OR). Picogreen dye (Molecular Probes) was added to the samples in duplicate in 96-well plates (100 μL dye:100 μL sample) and read in a fluorescent plate reader (Excitation 485 nm: emission 530 nm).

Protein and alkaline phosphatase—Tissue constructs were washed in PBS and then placed in 100 μL of lysate buffer (PBS, 1% Trition X-100, 0.5% sodium deoxycholate, 0.1% SDS, 0.1 mg/mL phenylmethylsulfonylfluoride, and 0.3% aprotinin). Samples were maintained on ice and vortexed every 30 min for up to 2 h to mechanically break down cell membranes. The extracts were removed and centrifuged and the supernatant stored at −20°C. For the protein assay, 10 μL of each sample was added to 200 μL of protein dye (Protein Assay,

BioRad, Hercules, CA) and the absorbance read at 595 nm. The readings were compared with a standard curve made using bovine serum albumin. For the alkaline phosphatase assay, 50 μL of samples was added to 50 μL of alkaline buffer and 50 μL of nitrophenyl-phosphate substrate solution in micro-centrifuge tubes at 37°C for 15 min. The reaction was stopped using 0.5 N sodium hydroxide solution. The absorbance was read at 405 nm and compared with a standard curve obtained from p-nitrophenol solutions of known concentrations.

Histology and immunohistochemistry—Constructs were washed in PBS and fixed in 10% formalin for 1 to 2 days. Samples were then decalcified for 2 days with Immunocal solution (Decal Chemical Corp., Tallman, NY), dehydrated with graded ethanol washes, embedded in paraffin, sectioned into 5-μm slices, and mounted on glass slides. (All four groups were processed in the same batch, with two sections per experimental group on each slide.) Samples were stained using conventional hematoxylin and eosin. Immunohistochemistry staining for collagen I, bone sialoprotein (BSP), and osteopontin were also performed. Briefly, the sections were deparaffinized with Citrisolv (Fisher, Pittsburgh, PA) and rehydrated with a graded series of ethanol washes. The antigens were retrieved by incubating in 0.25% trypsin. Sections were blocked with normal serum, stained with primary antibodies (collagen 1: mouse monoclonal anti-collagen I from Abcam (Cambridge, MA) (ab6308), BSP: rabbit polyclonal anti-BSP II from Chemicon (Temecula, CA) (AB1854), and osteopontin: rabbit polyclonal anti-osteopontin from Chemicon (AB1870)) and then secondary antibody, and developed with a biotin/avidin system. The serum, secondary antibody, and developing reagents were obtained from Vector Laboratories (Burlingame, CA) and included in the Vector Elite ABC kit (universal) (PK6200) and DAB/Ni Substrate (SK-4100). For negative controls, the first antibody incubation step was omitted.

Scanning electron microscopy—Samples were washed in PBS and then fixed in 2% glutaraldehyde in sodium cacodylate buffer for 2 h. Constructs were washed in buffer and freeze-dried overnight in a lyophilizer. Before imaging, samples were coated with gold and palladium and used for SEM. One construct from each group was used to image the cut surface, and another was used to image the outer surface.

Micro-computerized tomography—μCT was performed using a protocol described in detail in Liu *et al.*[30] with the following settings: voltage 55 kV, current 0.109 mA, slice thickness 21 μm, and inter-slice spacing 22 μm. After fixation with glutaraldehyde, the samples were aligned along their axial direction and stabilized with wet gauze in a 15-mL centrifuge tube. The tube was clamped in the specimen holder of a vivaCT 40 system (SCANCO Medical AG, Basserdorf, Switzerland). The 4-mm length of the scaffold was scanned at 21 μm isotropic resolution. The bone volume was obtained using a global thresholding technique that was applied to binarize gray-scale μCT images, and the minimum between the peaks in the voxel gray values histogram was chosen as the threshold value. The bone volume fraction (BVF) was calculated by dividing the bone volume by the volume of the sample. Spatial resolution of this full-voxel model was considered sufficient for evaluating the micro-architecture of the samples, based on the previously established methods.[30]

Statistical analysis

Pair-wise comparisons of results were carried out using multi-variate analysis of variance followed by Tukey's post hoc analysis using STATISTICA software (StatSoft Inc., Tusca, OK). $P < 0.05$ was considered significant.

RESULTS

Medium flow and shear stress within tissue constructs

The flow channels in the bioreactor provided an even distribution of medium flow between the six scaffolds. When scaffolds (n = 9) with densities ranging from 0.30 to 0.49 mg/ml were individually placed in the bioreactor, the flow rate through each scaffold for a constant pressure head remained 0.85 ± 0.01 mL/s regardless of density. By comparing flow through the bioreactor with and without all six scaffolds in place, at high pressure drop, the flow rate in each of the six channels measured 0.161 ± 0.001 mL/s (scaffolds in place) and 0.161 ± 0.002 mL/s (empty wells). At low pressure drop, the values were 0.0695 ± 0.001 mL/s (scaffolds in place) and 0.0698 ± 0.001 ML/s (empty wells). All measurements were repeated five times.

Order-of-magnitude estimates for shear stresses associated with medium flow in tissue constructs were obtained by making several assumptions. The internal geometries of the scaffolds were simplified by representing the porous network as bundles of cylindrical tubes of a given diameter (Fig. 2A). The complex architecture of the bone was represented using three simplified geometric configurations, all of which were modeled for the void volume of 70%, and fully developed laminar flow, as follows: First, to obtain the absolute minimum of the shear stress, the bone was modeled as a single 3.4-mm-diameter channel (calculated as combined void volume of the bone sample) within an outer cylinder. Next, the scaffold was represented as a system with 10 channels, 1.1 mm in diameter. Finally, the scaffold was modeled for a system containing 125 channels 300 μm in diameter each (which is considerably smaller than the pore sizes in DCB because tortuosity of the system is being neglected). The density (ρ) and viscosity (μ) values for culture medium were obtained from the literature as 1.004 g/mL and 0.77 cP, respectively.[29] The values for wall shear stresses (τ_w) were calculated as a function of cylinder diameter (d_c) and mean linear flow rate (u), using the equation $\tau_w = (8\ \mu u)/d_c$ derived from the Hagen-Poiseuille relation for laminar flow through a conduit. Reynolds numbers were calculated for each configuration to validate the assumption of laminar flow. The results of modeling in Figure 2B show the estimated shear stress as a function of the channel diameter and medium flow rate. For the conditions studied, the estimated levels of shear stress were between 0.7 and 10 mPa.

Scaffold properties

Native trabecular bovine bone was effectively decellularized by combining physical washing with detergent and enzymatic treatments. An average 6×10^5 cells per scaffold was measured for native bone (Fig. 3A). This corresponds to a cell density of 1.2×10^7 cells/mL of tissue, approximately ten times lower than typical values for native tissues, which may be due to high extracellular matrix (ECM) content in the bone marrow and the inability to fully digest the mineral encasing osteocytes (Fig. 3B). Also, the cellularity of the bone is heavily dependent on the age, the site of harvest, and the distance from the articular surface, resulting in large standard deviations of the DNA content of scaffolds. Pico-green assays indicated that washing the cored bone matrix removed roughly 80% of cells (Fig. 3A). Histological analysis indicated that osteocytes mostly remained trapped in the mineralized portion of the bone (Fig. 3C). Subsequent treatment methods removed an additional 98% of cells—including the osteocytes—resulting in virtually acellular scaffolds (Fig. 3D). Regardless of initial cell content, the decellularization procedure resulted in greater than 99.6% efficiency, with low standard deviations in the DNA content of processed bone scaffolds. The remaining components were primarily mineralized matrix and collagenous material and were found to have no apparent inflammatory or immunogenic responses after subcutaneous implantation into immuno-competent Sprague-Dawley rats. The decellularized scaffolds had approximately 70% to 80% void volume, with large pores approximately 600 to 1000 μm in diameter.

Cell distribution after seeding

For the LS-LF and LS-HF groups, a total of 1.5×10^6 cells were seeded into the scaffolds. Immediately after seeding, 3.5×10^5 cells per scaffold (28.1% of the total cells) were retained in the LS group (Fig. 3A), and 7.4×10^5 cells per scaffold (24.7% of the total cells) were retained in the HS group (Fig. 3A). Seeding efficiency was thus independent of the initial density for the two cell densities used in the experiment. The cells that remained in the scaffolds after seeding were well distributed throughout the scaffold (Fig. 3E). The hMSCs appeared as clusters of cells at the edges and in the central regions, rather than being homogenously dispersed throughout the matrix. This contrasts with the distribution of cells at the end of the culture period.

Cell distribution after cultivation

Histological staining of the cell constructs in all of the seeded groups revealed acellular regions throughout the central parts of the grafts (Fig. 4A). A cross-section of the constructs in the axial direction exhibited a “shell” of cellular material at the upper and lower faces, as well as along the walls of the cylinders. The thickness of the cellular layer along the sides of the scaffolds appeared to be similar in all groups. However, cell distribution into the scaffold from the upper and lower ends and morphology throughout the scaffolds appeared to be dependent on the flow-rate and initial seeding density. The thicknesses of the cellular regions in the HS-LF group were estimated to be approximately 350 μm (Fig. 4A) and approximately 500 μm in LS-LF, whereas that of the high flow-rate (LS-HF) group was approximately 800 μm and approaching 1 mm from the edge in some places. At higher magnifications, however, another major difference was apparent in the two LF groups; the LS-LF group had thicker cell growth, but the cell density and ECM deposition were low, whereas the HS-LF group had a thin shell but densely packed cellular material (Fig. 4B). (The DNA values for the two groups are similar.) The cells in the HF groups exhibited dense packing as well as enhanced growth into the scaffolds.

Cell morphology

Low-magnification (30×) images of the external surfaces of the seeded scaffolds indicated that hMSCs formed dense structures in the trabecular spaces (Fig. 4C). Examining the cut surfaces at higher magnifications (1000×) illustrated the formation of fibrillar ECM networks by the cells and demonstrated cells embedding themselves into the extra-cellular proteins (Fig. 4D). The large, empty pores at the beginning of culture would indicate that cells could adhere only to the walls of the pore spaces. However, by creating ECM networks and growing into the pore spaces, cells were able to provide themselves with a 3D context in localized regions.

Mineral deposition in engineered bone

Image analysis using μ-CT demonstrated that there were some differences in the microstructure of the bone grafts even after the cultivation period (Fig. 4E). All seeded groups exhibited greater bone volume fractions than the unseeded group. The BVF of the seeded groups was approximately 4% greater than that of the unseeded controls. The unseeded scaffolds had a BVF of 20%, whereas the volume fractions of the seeded groups ranged from 23.8% to 24.5%. Two other parameters were examined: connectivity density (a measure of the number of trabeculae that need to be cut in a given volume before the scaffolds break into two) and trabeculae number (the number of trabeculae per unit length). The average values for the unseeded scaffolds were 4.45 mm^{-3} and 2.10 mm^{-1} respectively (Table 1). These values increased gradually: LS-LF (4.48 mm^{-3}, 2.21 mm^{-1}), LS-HF (5.78 mm^{-3}, 2.28 mm^{-1}), and HS-LF (6.34 mm^{-3}, 2.35 mm^{-1}).

Biochemical composition of engineered bone

As expected, the seeded groups had statistically higher values for dry and wet weight (not shown), total protein, alkaline phosphatase, DNA, and BVF than unseeded scaffolds (Fig. 5A–D, respectively). However, the only statistical differences between the seeded groups were in the DNA values; the high-flow-rate (LS-HF) group facilitated higher cell numbers than either of the low-flow-rate groups. The DNA values (given as ngDNA/mg wet weight) corresponding to cell numbers in the LS-HF, LS-LF, and HS-LF groups that were 81.0%, 36.8%, and 23.2% of day 0 values, respectively.

Expression of bone markers

Cell constructs from each group were stained with antibodies to BSP, collagen I, and osteopontin that are all indicative of osteogenic differentiation (Fig. 5E). Unseeded constructs did not stain for BSP and osteopontin, but as expected, the mineralized regions of unseeded constructs stained positively for collagen I. The cellular regions of seeded constructs stained positively for collagen I, BSP, and osteopontin (not shown) content.

DISCUSSION

Perfusion bioreactor system

We describe a novel perfusion system capable of culturing up to six tissue constructs simultaneously, thus enabling the collection of sufficient data for statistical analysis of each set of conditions (Fig. 1). The bioreactor design provided equal flow rates in the six individual scaffolds, for a wide range of flow rates (up to 1 mL/s of total flow) and scaffold densities (0.30–0.49 mg/mL). Even if the culture wells were empty (scaffold-free), the individual flow rates remained at the same level for a given pressure head. This feature is based on a higher flow resistance in the bioreactor channels than in the rest of the system and is important for preventing uneven distribution of flow due to the changes in scaffold density during cultivation. The system can also be modified in different ways. The scaffolds used in this study were 4 mm high×4 mm in diameter. However, the bioreactor can be easily modified to culture cylindrical pieces of various diameters and thicknesses by having just one interchangeable layer with different well sizes. Another major advantage of the system is its ease of operation, acting, in essence, as a functionalized Petri dish. The system has the potential for online monitoring of bone growth and mineral deposition because scaffolds can be removed sterilely, imaged using non-invasive techniques such as nuclear magnetic resonance or μ-CT, and replaced. In these experiments, cell-seeded scaffolds were press-fit into the wells of the bioreactor with a surrounding gasket (made from PDMS), and flow experiments demonstrated that perfusion occurred through the interstices of the scaffolds rather than around its periphery.

Decellularized trabecular bone as a tissue-engineering scaffold

Functional bone grafts can be generated by seeding suitable biomaterial scaffolds with cells that have osteogenic potential and culturing them under conditions that optimize their bone-forming capabilities. Scaffolds should not exhibit immunogenic properties. For native tissues, this requires the effective removal of all cellular components and immunogenic proteins. In the present study, decellularization of bovine bone constructs resulted in the lack of invading leukocytes into scaffolds implanted subcutaneously into immuno-competent rats. From a tissue-engineering perspective, the topography of the scaffolds, as well as pore size, pore distribution, and biochemical content, should present hMSCs with a highly osteogenic microenvironment. Previous studies have shown that the presence of mineral in the constructs does not enhance or inhibit osteogenesis of hMSCs relative to demineralized bone constructs, [27] suggesting that growth factors trapped within the matrix remain accessible to hMSCs and

that the mineral component does not enhance osteogenesis in hMSCs significantly better than in non-mineralized scaffolds.

Influence of seeding density and flow-rate

There were some, but not major, differences between the high-seeding-density and low-seeding-density groups (LS-LF and HS-LF) at the end of 5 weeks of culture with respect to the quantifiable parameters. Whereas the μ-CT analysis suggested differences in the microstructure of new bone formation (Fig. 5, Table 1), the histological analysis (Fig. 4, 5) indicated differences in cell distributions, cell morphologies, and ECM deposition. Hence, the initial seeding density may influence the cellular development in the resulting bone graft but does not appear to enhance bone formation or final cellular content. Comparisons with prior studies[19] suggest that the effect of increasing cell numbers is apparent only at lower seeding densities and may be widely negated in these experiments in which the seeding densities in the LS and HS groups were both high.

Conversely, flow rate appeared to play a more-significant role in the growth and tissue development of hMSCs within the scaffolds. The flow rates for the experiments were chosen to be within the ranges of superficial velocities used in other studies, in which considerable differences in mineral deposition were noted for variations in perfusion rates.[5,10,31] The LS-HF group had twice as many cells as either of the low-flow-rate groups (Fig. 3A). This correlated with the findings in histology, which showed that the thickness and densities of the cellular regions were also considerably higher in LS-HF than in the other seeded groups (Fig. 4A, B). However, other measurable parameters, for example protein and BVF (Fig. 5B, D, respectively), were only slightly higher in the LS-HF group and not statistically different from in the low-flow groups. This suggests that the major advantage of high flow is better maintenance of cells rather than stimulation to form more mineralized deposits. To further support this, cell numbers at the end of the culture period were lower than at day 0 (Fig. 5C), suggesting that the differences were due to higher survival rates rather than enhanced proliferation of cells.

Oxygen becomes severely limiting for cells cultured statically within 3D matrices;[1] hence, medium perfusion is necessary to enhance cell survival.[2,32] In this study, it appeared that increased nutrient transport from higher perfusion rates may be the primary factor contributing to differences observed between experimental groups. However, medium perfusion imparts fluid shear stresses to cells, and the shear levels within the system should be optimized for cell growth. A study done by Cartmell *et al.*[8] showed that low perfusion rates (0.01 mL/min) resulted in significantly greater osteoblast-like cell expansion than in static controls, whereas there was a decrease in cell viability within the constructs corresponding with increases in flow rates from 0.01 mL/min to 1.0 mL/min. In contrast, another group investigating the effects of perfusion rates on rat marrow-stromal osteoblasts found that greater flow rates (0.3, 1.0 and 3.0 mL/min) enhanced mineralization and calcium deposition in a dose-dependent manner. These inconsistencies may be explained in terms of differences in cell types, but differences in system geometries and internal architectures of the scaffolds such that similar volumetric flow rates result in highly dissimilar shear stresses imparted to cells also complicate direct comparisons. To aid in comparisons, flow rates in this study are reported as superficial linear velocities.

For the flow rates used, estimates of shear stresses within the constructs ranged from 0.0007 Pa (d_c = 1100 μm) to 0.01 Pa (d_c = 300 μm) (Fig. 2B). These values are similar to those reported in the literature for 3D scaffold systems.[33,34] However, they are up to one thousand times lower than the shear levels required to elicit measurable responses from osteoblasts[7,35] seeded on 2D surfaces or those predicted to act on osteocytes trapped in the lacuna system of native bone.[36] It is also roughly ten times lower than other *in vitro* studies designed specifically to elucidate

the role of shear on bone formation in 3D scaffolds.[31] However, the approach used only gives order of magnitude estimates and does not account for the increases in shear with changes in internal architecture due to ECM deposition and mineralization. Hence, the role of shear in maintaining higher cell numbers and affecting osteogenesis in this system is not entirely clear, and further studies are ongoing to determine its role in tissue development.

Patterns of tissue development

In the engineering of a specific tissue phenotype, it is widely assumed that the eventual functionality is directly correlated with homogenous cell growth and matrix formation throughout the construct. One of the major motivations for using direct perfusion is to facilitate the uniform development of the tissue constructs. However, the growth patterns observed in these studies show cells developing preferentially on the edges of tissue constructs, as well as the inlet and outlet regions of the construct cross-section. This pattern is also observed in the mineralization data of perfusion studies performed by other groups.[8] One assumption is that, as cells grow into the pore spaces, they begin to occlude flow through the constructs and medium flows around the DCB scaffolds. However, the scaffolds are tightly press-fit into PDMS gaskets of a slightly smaller diameter, making it unlikely that fluid flows around the periphery rather than through the interstitial spaces, even at later stages of culture. The thicknesses of the cellular layers at the inlets and outlets correlate with perfusion rates, further suggesting that medium continues to perfuse through the interstices (Fig. 5E). The low-density central regions of constructs may therefore be indicative of insufficient nutrient delivery and may be solved by using even higher flow rates, the work now in progress.

CONCLUSION

This study describes the development and use of a versatile perfusion system in combination with decellularized bovine trabecular bone scaffolds to study the relative effects of greater seeding densities of hMSCs and higher medium perfusion rates. The results of the study indicate that, at the seeding densities evaluated, greater initial cell numbers do not necessarily result in increased bone formation. The flow rate of medium perfusion remains a significant parameter because the better nutrient transport afforded by higher perfusion rates enables more-uniform tissue development and supports higher cell densities within the constructs. Because the levels of shear stress are low in the range of flow rates studied, future studies need to investigate the ability of even higher perfusion rates to support cell growth throughout the 4-mm thickness of the scaffolds and determine at which point higher flow becomes detrimental to construct development.

Acknowledgments

The authors would like to thank Dr. Ed Guo for kindly sharing his μCT system and imaging expertise and Dr. Timothy Martens for help with animal surgery. The study was funded by the National Institutes of Health (R01 DE161525-01 and P41 EB02520-01A1, GV-N), Arthritis Foundation (PG Chao), and the Mandl Foundation (WG).

References

1. Martin I, Wendt D, Heberer M. The role of bioreactors in tissue engineering. Trends Biotechnol 2004;22:80. [PubMed: 14757042]
2. Coletti F, Macchietto S, Elvassore N. Mathematical modeling of three-dimensional cell cultures in perfusion bioreactors. Ind Eng Chem Res 2006;45:8158.
3. Griffith LG, Swartz MA. Capturing complex 3D tissue physiology *in vitro*. Nat Rev Mol Cell Biol 2006;7:211. [PubMed: 16496023]
4. Bancroft GN, Sikavitsas VI, Mikos AG. Design of a flow perfusion bioreactor system for bone tissue-engineering applications. Tissue Eng 2003;9:549. [PubMed: 12857422]

5. Bancroft GN, Sikavitsast VI, van den Dolder J, Sheffield TL, Ambrose CG, Jansen JA, Mikos AG. Fluid flow increases mineralized matrix deposition in 3D perfusion culture of marrow stromal osteloblasts in a dose-dependent manner. Proc Natl Acad Sci U S A 2002;99:12600. [PubMed: 12242339]
6. Botchwey EA, Dupree MA, Pollack SR, Levine EM, Laurencin CT. Tissue engineered bone: Measurement of nutrient transport in three-dimensional matrices. J Biomed Mater Res A 2003;67:357. [PubMed: 14517896]
7. Botchwey EA, Pollack SR, El-Amin S, Levine EM, Tuan RS, Laurencin CT. Human osteoblast-like cells in three-dimensional culture with fluid flow. Biorheology 2003;40:299. [PubMed: 12454419]
8. Cartmell SH, Porter BD, Garcia AJ, Guldberg RE. Effects of medium perfusion rate on cell-seeded three-dimensional bone constructs *in vitro*. Tissue Eng 2003;9:1197. [PubMed: 14670107]
9. Holtorf HL, Jansen JA, Mikos AG. Flow perfusion culture induces the osteoblastic differentiation of marrow stromal cell-scaffold constructs in the absence of dexamethasone. J Biomed Mater Res A 2005;72:326. [PubMed: 15657936]
10. Sikavitsas VI, Bancroft GN, Holtorf HL, Jansen JA, Mikos AG. Mineralized matrix deposition by marrow stromal osteoblasts in 3D perfusion culture increases with increasing fluid shear forces. Proc Natl Acad Sci U S A 2003;100:14683. [PubMed: 14657343]
11. Yu XJ, Botchwey EA, Levine EM, Pollack SR, Laurencin CT. Bioreactor-based bone tissue engineering: The influence of dynamic flow on osteoblast phenotypic expression and matrix mineralization. Proc Natl Acad Sci U S A 2004;101:11203. [PubMed: 15277663]
12. Glowacki J, Mizuno S, Greenberger JS. Perfusion enhances functions of bone marrow stromal cells in three-dimensional culture. Cell Transplant 1998;7:319. [PubMed: 9647441]
13. Rubin J, Rubin C, Jacobs CR. Molecular pathways mediating mechanical signaling in bone. Gene 2006;367:1. [PubMed: 16361069]
14. Donahue TLH, Haut TR, Yellowley CE, Donahue HJ, Jacobs CR. Mechanosensitivity of bone cells to oscillating fluid flow induced shear stress may be modulated by chemotransport. J Biomech 2003;36:1363. [PubMed: 12893045]
15. Jacobs CR, Yellowley CE, Davis BR, Zhou Z, Cimbala JM, Donahue HJ. Differential effect of steady versus oscillating flow on bone cells. J Biomech 1998;31:969. [PubMed: 9880053]
16. Saini S, Wick TM. Concentric cylinder bioreactor for production of tissue engineered cartilage: effect of seeding density and hydrodynamic loading on construct development. Biotechnol Prog 2003;19:510. [PubMed: 12675595]
17. Wilson CE, Dhert WJA, Van Blitterswijk CA, Verbout AJ, De Bruijn JD. Evaluating 3D bone tissue engineered constructs with different seeding densities using the alamarBlue (TM) assay and the effect on *in vivo* bone formation. J Mater Sci Mater Med 2002;13:1265. [PubMed: 15348675]
18. Mauck RL, Nicoll SB, Stark R, Hung CT, Ateshian GA. Joint-specific surface molds for articular cartilage tissue engineering. Trans Orthop Res Soc 2002;27:251.
19. Holy CE, Shoichet MS, Davies JE. Engineering three-dimensional bone tissue *in vitro* using biodegradable scaffolds: investigating initial cell-seeding density and culture period. J Biomed Mater Res 2000;51:376. [PubMed: 10880079]
20. Carrier RL, Papadaki M, Rupnick M, Schoen FJ, Bursac N, Langer R, Freed LE, Vunjak-Novakovic G. Cardiac tissue engineering: cell seeding, cultivation parameters, and tissue construct characterization. Biotechnol Bioeng 1999;64:580. [PubMed: 10404238]
21. Urist MR. Bone-formation by autoinduction. Science 1965;150:893. [PubMed: 5319761]
22. Urist MR, Delange RJ, Finerman GAM. Bone cell differentiation and growth factors. Science 1983;220:680. [PubMed: 6403986]
23. De Long WG, Einhorn TA, Koval K, McKee M, Smith W, Sanders R, Watson T. Bone, grafts and bone graft substitutes in orthopedic trauma surgery—a critical analysis. J Bone Joint Surg Am 2007;89A:649. [PubMed: 17332116]
24. Takai E, Lima EG, Lu HH, Ateshian GA, Guo XE, Hung CT. Devitalized bone as a mineralized substrate for osteochondral tissue engineered hydrogel constructs. Trans Orthop Res Soc 2003;28:307.
25. Lima EG, Mauck RL, Han SH, Park S, Ng KW, Ateshian GA, Hung CT. Functional tissue engineering of chondral and osteochondral constructs. Biorheology 2004;41:577. [PubMed: 15299288]

26. Hung CT, Lima EG, Mauck RL, Taki E, LeRoux MA, Lu HH, Stark RG, Guo XE, Ateshian GA. Anatomically shaped osteochondral constructs for articular cartilage repair. J Biomech 2003;36:1853. [PubMed: 14614939]
27. Mauney JR, Jaquiery C, Volloch V, Herberer M, Martin I, Kaplan DL. *In vitro* and *in vivo* evaluation of differentially demineralized cancellous bone scaffolds combined with human bone marrow stromal cells for tissue engineering. Biomaterials 2005;26:3173. [PubMed: 15603812]
28. Lennon DP, Caplan AI. Isolation of human marrow-derived mesenchymal stem cells. Exp Hematol 2006;34:1604. [PubMed: 17046583]
29. Moreira JL, Santana PC, Feliciano AS, Cruz PE, Racher AJ, Griffiths JB, Carrondo MJT. Effect of viscosity upon hydrodynamically controlled natural aggregates of animal-cells grown in stirred vessels. Biotechnol Prog 1995;11:575. [PubMed: 8546840]
30. Liu XWS, Sajda P, Saha PK, Wehrli FW, Guo XE. Quantification of the roles of trabecular microarchitecture and trabecular type in determining the elastic modulus of human trabecular bone. J Bone Miner Res 2006;21:1608. [PubMed: 16995816]
31. Sikavitsas VI, Bancroft GN, Lemoine JJ, Liebschner MAK, Dauner M, Mikos AG. Flow perfusion enhances the calcified matrix deposition of marrow stromal cells in biodegradable nonwoven fiber mesh scaffolds. Ann Biomed Eng 2005;33:63. [PubMed: 15709706]
32. Pathi P, Ma T, Locke BR. Role of nutrient supply on cell growth in bioreactor design for tissue engineering of hematopoietic cells. Biotechnol Bioeng 2005;89:743. [PubMed: 15696509]
33. Porter B, Zauel R, Stockman H, Guldberg R, Fyhrie D. 3-D computational modeling of media flow through scaffolds in a perfusion bioreactor. J Biomech 2005;38:543. [PubMed: 15652553]
34. Boschetti F, Raimondi MT, Mighavacca F, Dubini G. Prediction of the micro-fluid dynamic environment imposed to three-dimensional engineered cell systems in bioreactors. J Biomech 2006;39:418. [PubMed: 16389082]
35. Donahue SW, Jacobs CR, Donahue HJ. Flow-induced calcium oscillations in rat osteoblasts are age, loading frequency, and shear stress dependent. Am J Physiol Cell Physiol 2001;281:C1635. [PubMed: 11600427]
36. Zeng Y, Cowin SC, Weinbaum S. A Fiber-matrix model for fluid-flow and streaming potentials in the canaliculi of an osteon. Ann Biomed Eng 1994;22:280. [PubMed: 7978549]

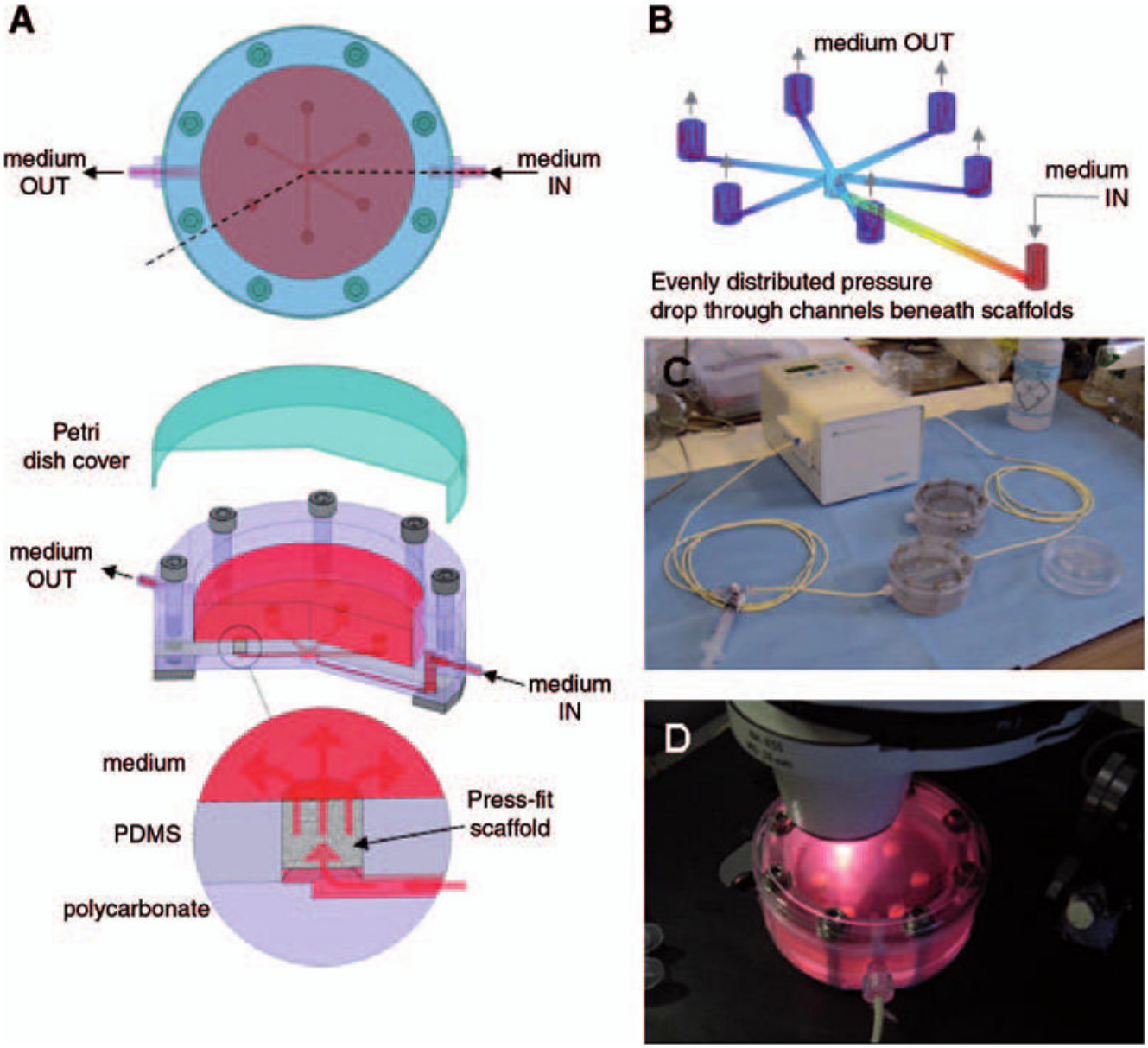

FIG. 1.

Bioreactor design. (**A**) Schematic presentation of the bioreactor system used to provide perfusion through six cell-seeded scaffolds that were press-fit into the culture wells. Scaffolds were 4-mm-diameter×4-mm-high plugs of fully decellularized, mineralized bone. (**B**) Computational Fluid Dynamics simulation of flow through channels indicating uniform flow to all six wells. (**C**) Complete experimental set-up showing bioreactor, perfusion loop, and peristaltic pump. (**D**) Bioreactor on a microscope stage during imaging of tissue constructs *in situ*. Color images available online at www.liebertonline.com/ten.

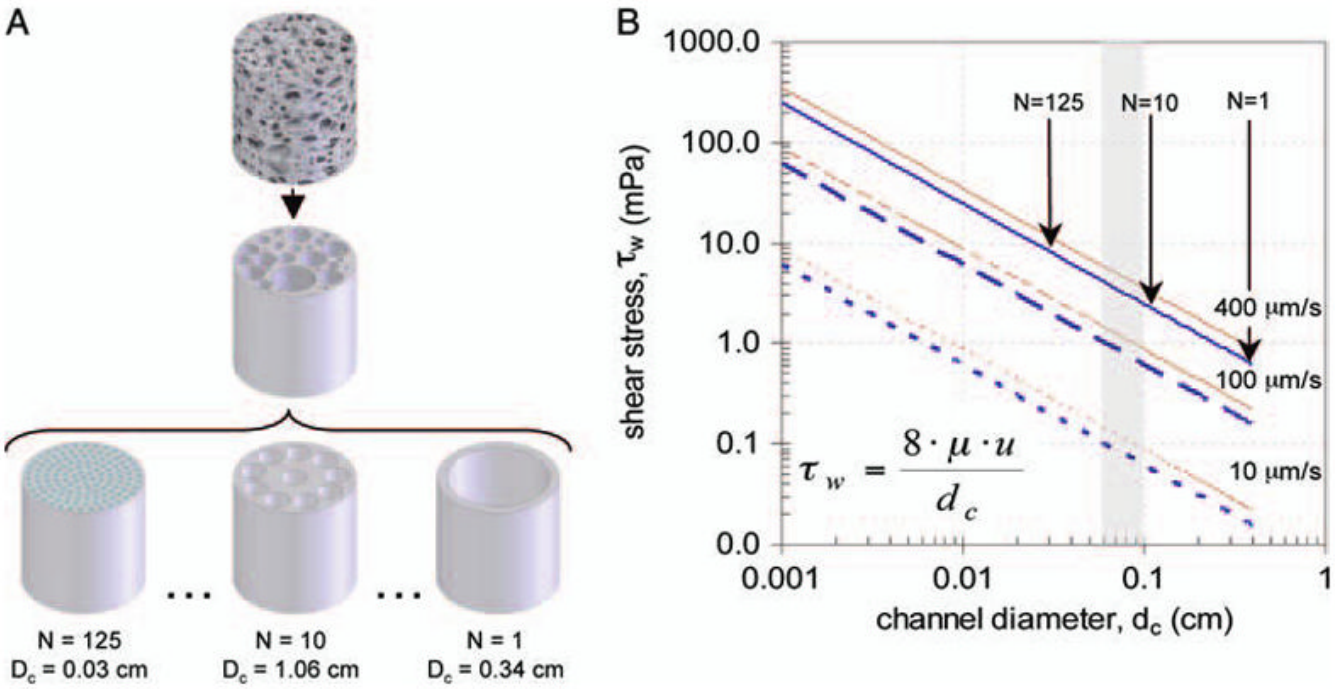

FIG. 2.

Estimates of shear stress in decellularized bone scaffolds. (**A**) The complex bone scaffold geometry was simplified by reducing the interconnected pore network to a bundle of parallel, cylindrical channels of varying diameters in order to estimate the shear rates. The number of channels were adjusted so that the linear velocities were equal in all cases. (**B**) Wall shear as a function of pore diameter and medium flow rate. Lines indicate shear values for constant linear flow rates through a scaffold 4 mm in diameter (blue) and corrected for 70% scaffold void volume (red) while varying the number of tubes. Gray area indicates range of estimated pore sizes from micro computed tomography analysis of scaffolds. Color images available online at www.liebertonline.com/ten.

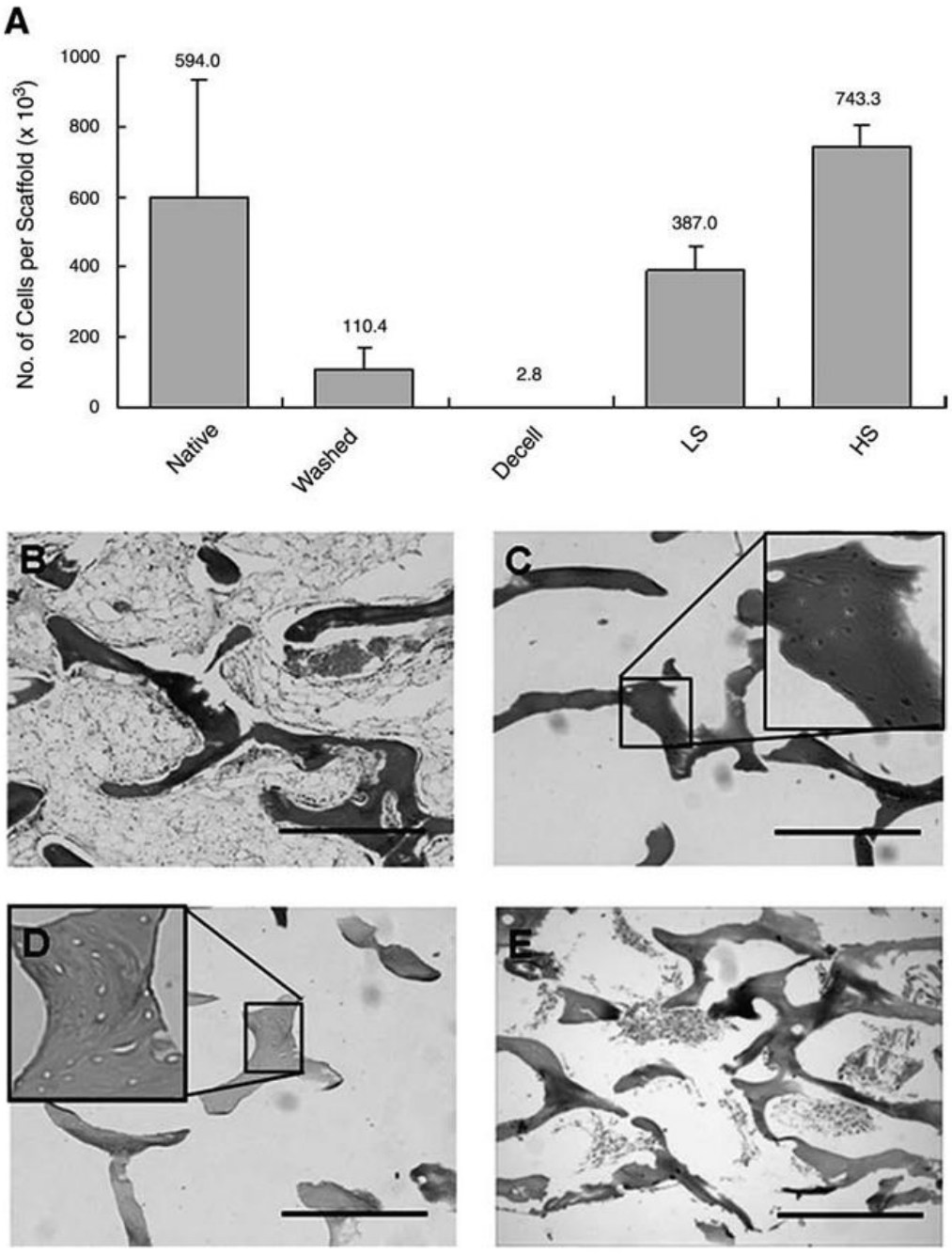

FIG. 3.

Decellularized bone scaffold. (**A**) DNA content of native bone at various stages of preparation and after seeding with cells. (**B)–(E**) Hematoxylin and eosin staining of the native bone and bone scaffold. (**B**) Native trabecular bone. (**C**) Trabecular bone after washing with a high-pressure stream of water. Osteocytes are visible in the lacunae of the mineralized regions. (**D**) Trabecular bone after entire decellularization process showing that osteocytes are removed. (**E**) Central region of re-seeded bone scaffolds showing cell distribution in the pore spaces. LS, low seeding density; HS, high seeding density.

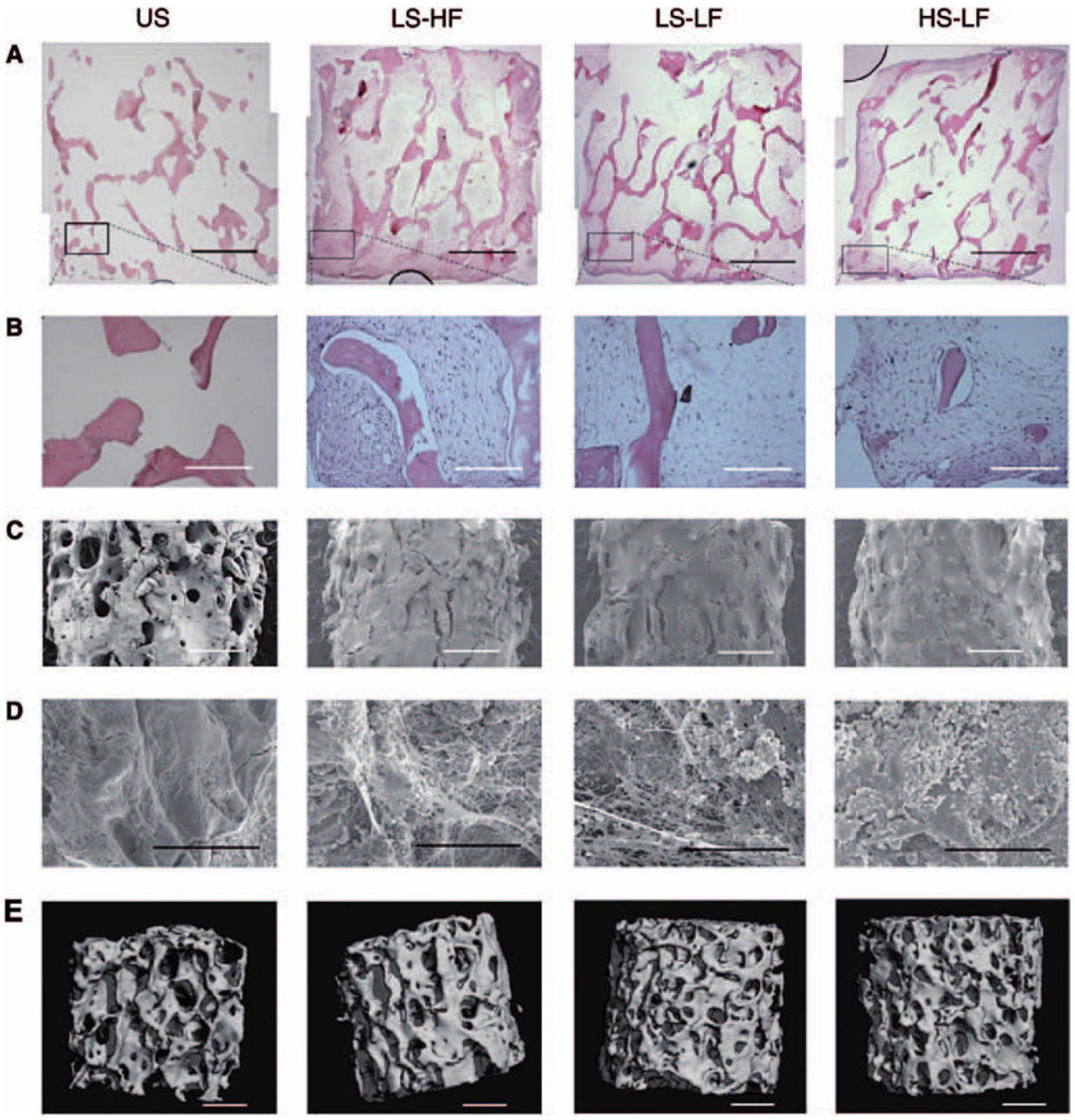

FIG. 4.

Tissue engineered bone: morphology. (**A**) Hematoxylin and eosin staining of seeded scaffolds after 5 weeks of culture. Cells grow along the periphery of scaffolds in all groups. Uniformity is greatest in the low seeding density, high flow (LS-HF) group, where cells grow 800 μm or more into the scaffold from the upper and lower edges, and least in the high seeding density, low flow (HS-LF) group, with growth up to approximately 350 μm. (Scale bar = 1 mm) (**B**) Cell density in specific regions differs significantly between groups. The LS-HF and HS-LF groups have high localized cell densities, whereas the LS-LF group has low cell density (scale bar = 200 μm) (**C**) Low-magnification scanning electron microscopy (SEM) images (30×) of external surfaces of tissue constructs showing cell growth and extracellular matrix deposits in

seeded scaffolds (scale bar = 1 mm). (**D**) High-magnification SEM images (1000×) of inner regions showing cell interaction with the mineralized walls and formation of three-dimensional networks in the seeded groups (scale bar = 50 μm). (**E**) Micro computed tomography images of tissue constructs from all groups after 5 weeks of culture (scale bar = 1 mm). Color images available online at www.liebertonline.com/ten.

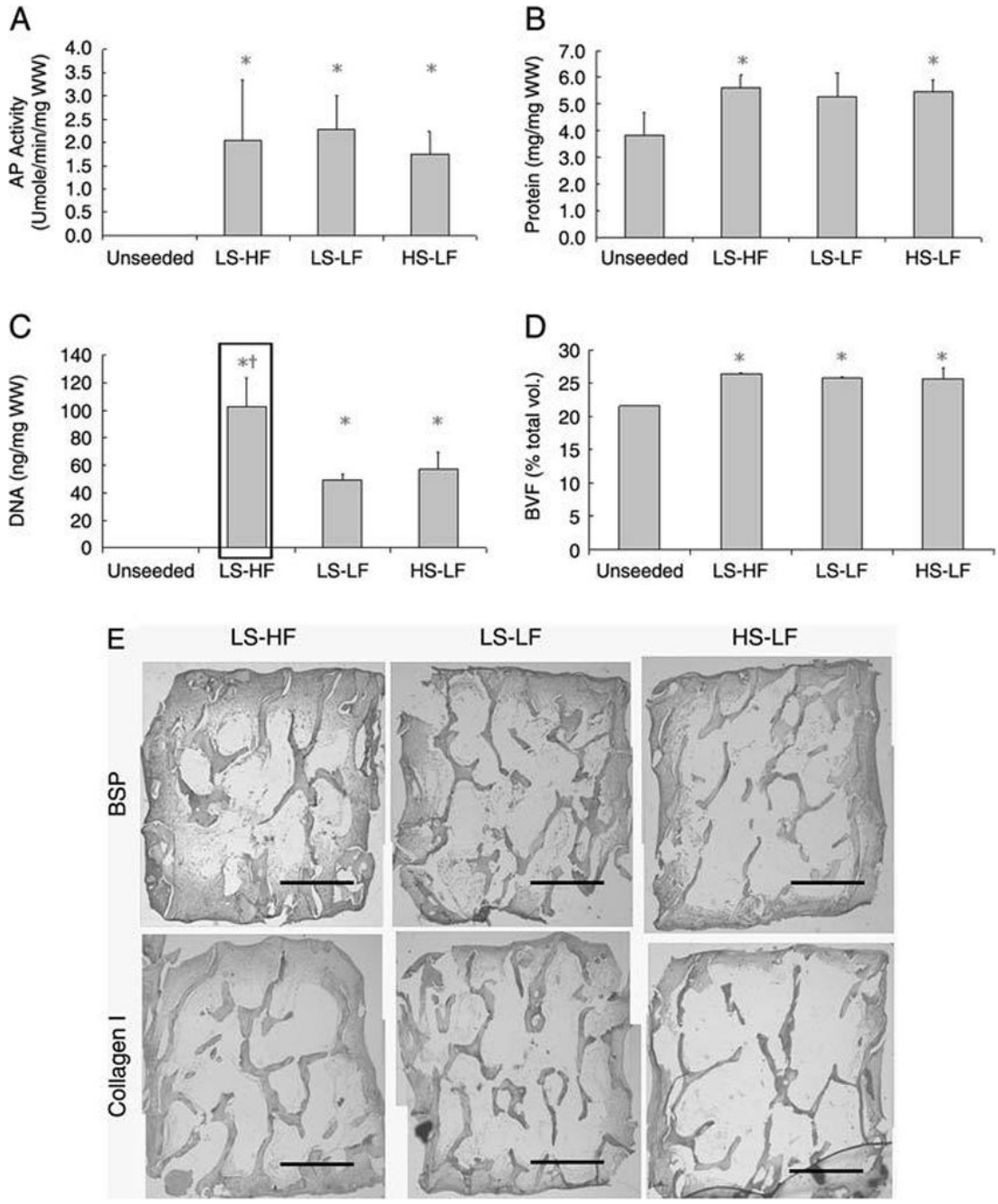

FIG. 5.

Tissue-engineered bone: marker expression. **(A)** Alkaline phosphatase activity of cells within the tissue constructs. (**B**) Total protein content. (**C**) DNA content. (**D**) Bone volume fractions. (n = 4 per group; *statistically different from unseeded group; †statistically different from all other groups). (**E**) Expression of bone sialoprotein and collagen I after 5 weeks of culture (scale bar = 1 mm).

Table 1

Micro-CT Analysis of Scaffolds after 5 Weeks of Cultivation

Group	Connectivity Density (mm^{-3})	Trabeculae No. (mm^{-1})
US	4.45 ± 1.50	2.10 ± 0.15
LS-HF	5.77 ± 0.76	2.28 ± 0.24
LS-LF	4.48 ± 0.96	2.21 ± 0.18
HS-LF	6.34 ± 1.27	2.35 ± 0.10